IEICE Electronics Express, Vol.16, No.12, 1–5

LETTER

Simplified pilot-aided weighted least square phase estimation method for OFDM-based WLANs

Xiaoping Zhou[1,2a)], Bin Wu[1], Kan Zheng[2], and Zhou Wang[1]

Abstract In this paper, we propose a simplified weighted least square (SWLS) to estimate phase variations utilizing pilots, for Orthogonal Frequency Division Multiplexing (OFDM) based very high throughput wireless local area networks (WLANs). For SWLS, the common phase error (CPE) maximum likelihood (ML) estimation and the angle boundary treatment are improved to enhance the performance of phase estimation, while the combined scheme of pair pilots is used to reduce the complexity. Simulation results show that, compared to weighted least square (WLS) scheme, a similar pocket error rate (PER) is achieved by using the SWLS method, but more than 40 percent of complexity is reduced.

Keywords: WLAN, phase estimation, CPE, WLS estimation
Classification: Integrated circuits

1. Introduction

Orthogonal Frequency Division Multiplexing (OFDM) has been deployed for many novel very high throughput wireless local area network (WLAN) standards such as 802.11n [1] and 802.11ac [2], mainly due to its robustness to frequency selective fading [3, 4].

It's well known that OFDM signal is very sensitive to the performance of synchronizer [5, 6, 7, 8, 9, 10], which is responsible for detecting the incoming frame, estimating and correcting the possible carrier frequency offset (CFO). However, residual CFO will be left after synchronization and the phase noise (PN) can't be compensated by synchronization either [11, 12]. Residual CFO and PN will cause phase rotation in frequency domain, which is common phase error (CPE). The CPE effect of PN is similar to the effect of mentioned residual CFO [13, 14], so no more separate consideration is taken. Besides, sampling frequency offset (SFO) will also introduce remaining phase, which is sampling time offset (STO) [15, 16]. In WLAN systems, the pilots, which are some known sub-carriers inside OFDM symbols, are used to estimate the remaining phase [17].

To compensate for the residual phase, several methods have been proposed. [18, 19, 20] introduced the ideal estimation, but it was too complex to implement. [21, 22] only dealt with the CPE and ignored the STO, resulting in performance degradation for long frame. An accurate STO estimation method was proposed in [23], neglecting the CPE, but it couldn't work in real WLAN systems because the residual CFO was not small enough [24]. [25] only calculated the CPE symbol by symbol, while the STO was obtained from the earlier CFO estimation, ignoring residual STO and resulting in performance losing. These are not suitable for WLAN systems.

In [26], least square (LS) method was presented, which was easy to implement. [27] improved a simplified residual phase correction mechanism (SRPCM), in which the linear phase could approximate to a nearly constant phase throughout the OFDM and the method could be significantly simplified, but with a poor performance. Based on the LS, [28] put forward weighted least square (WLS) to get better performance, leading to high computational complexity.

In this paper, we present a simplified weighted least square (SWLS) method to estimate the CPE and STO efficiently, which can achieve almost the same pocket error rate (PER) as WLS method. For SWLS, the CPE maximum likelihood (ML) estimation, the angle boundary treatment and the combined scheme of pair pilots are three key mechanisms. The CPE ML estimation and the angle boundary treatment are applied to ensure the performance. Meanwhile, the combined scheme of pair pilots is used to reduce the complexity.

The paper is organized as follows. In section 2, the residual phase model based on IEEE 802.11ac system is introduced. Section 3 presents the suggested phase estimation algorithm using pilots. The results of simulation to verify the scheme are provided in section 4. Finally, conclusion is presented in section 5.

2. Residual phase model

The effects of residual carrier frequency and sampling clock error are incorporated in the equivalent system model, as depicted in Fig. 1.

We consider an OFDM system using an inverse fast Fourier transform (IFFT) of size N for modulation. Each OFDM symbol is composed of $K < N$ data symbols $s_{l,k}$, where l denotes the OFDM symbol time index and k denotes the subcarrier frequency index. With the sampling time of $T = T_u/N$, where T_u is the useful symbol time, and proper filter $g_T(t)$, the transmitted baseband signal can be described as

[1]Institute of Microelectronics of Chinese Academy of Science, Beijing, China
[2]Beijing University of Posts and Telecommunications
a) zhouxiaoping@ime.ac.cn

DOI: 10.1587/elex.16.20190248
Received April 5, 2019
Accepted April 26, 2019
Publicized May 23, 2019
Copyedited June 25, 2019

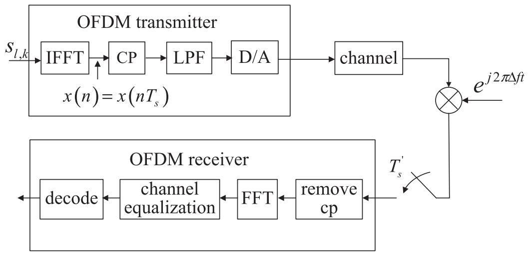

Fig. 1. Block diagram of an OFDM transmission chain

$$x(t) = \frac{1}{\sqrt{T_u}} \sum_{l=-\infty}^{+\infty} \sum_{k=-K/2}^{K/2} s_{l,k} \psi_{l,k}(t)^* g_T(t) \tag{1}$$

Taking into account of a guard interval of length T_g, the resulting subcarrier pulse is

$$\psi_{l,k}(t) = e^{j2\pi k/T_u(t-T_g-lT_s)} u(t - lT_s) \tag{2}$$

$$u(t) = \begin{cases} 1, & 0 \le t < T_s \\ 0, & else \end{cases} \tag{3}$$

where $T_s = T_u + T_g$ is the length of symbols.

The signal is transmitted over a frequency selective fading channel

$$h(\tau, t) = \sum_i h_i(t)\delta(\tau - \tau_i) \tag{4}$$

where $h_i(t)$ is the channel impulse response with the delay τ_i.

Assuming the receiver filter is flat within transmission bandwidth, the receiver signal is

$$r(t) = \sum_i h_i(t) \cdot x(t - \tau_i) + n(t) \tag{5}$$

where $n(t)$ is the additive white Gaussian noise (AWGN).

In the presence of a residual CFO Δf and a SFO of $\zeta = (T' - T)/T$, the sampled signal at time instant $t_n = nT' = n(1+\zeta)T$ is

$$\begin{aligned} r(t_n) &= e^{j2\pi\Delta f(nT')} \sum_i h_i(nT')x(nT' - \tau_i) + n(nT') \\ &= e^{j2\pi\Delta f(n(1+\zeta)T)} \sum_i h_i(n(1+\zeta)T)x(n(1+\zeta)T - \tau_i) \\ &\quad + n(n(1+\zeta)T) \end{aligned} \tag{6}$$

where T' is the sampling time at receiver, $x(nT' - \tau_i)$ and $x(n(1+\zeta)T - \tau_i)$ denote the sampling of signal $x(t)$, $h_i(nT')$ and $h_i(n(1+\zeta)T)$ denote the sampling of channel impulse response $h_i(t)$, $n(nT')$ and $n(n(1+\zeta)T)$ are the sampling of noise $n(t)$.

We assume an abbreviation $n' = n + N_g + lN_s$, and the received samples at time instant $t_{n'} = n'T' = n'(1+\zeta)T$ can be further expanded to yield

$$\begin{aligned} r_{l,n} &= r(t_{n'}) = e^{j2\pi\Delta f(n'(1+\zeta)T)} \sum_i h_i(n'(1+\zeta)T)x(n'(1+\zeta)T - \tau_i) \\ &+ n(n'(1+\zeta)T) = e^{j2\pi\Delta f n'T(1+\zeta)} \left(\sum_i h_i \sum_l \sum_k s_{l,k}\psi(n'T(1+\zeta) - \tau_i) \right) \\ &+ n_{l,n} \end{aligned} \tag{7}$$

where we have $\psi(n'T(1+\zeta) - \tau_i) = e^{j2\pi(\frac{k}{N})(n'(1+\zeta)-N_g-lN_s-\frac{\tau_i}{T})}$ $u((n'(1+\zeta) - lN_s - \tau_i))$ and $n_{l,n}$ is the noise.

In the absence of inter symbol interference (ISI), the *lth* received signal block r_l could be demodulated by fast Fourier transform (FFT)

$$\begin{aligned} z_{l,k} &= (e^{j\pi\phi_k} e^{j2\pi((lN_s+N_g)/N)\phi_k}) si(\pi\phi_k) s_{l,k} H_k \\ &\quad + \underbrace{\sum_{i,i\neq k} (e^{j\pi\phi_{i,k}} e^{j2\pi((lN_s+N_g)/N)\phi_i}) si(\pi\phi_{i,k}) s_{l,i} H_i + n_{l,k}}_{ICI} \end{aligned} \tag{8}$$

with cross-subcarrier and subcarrier local frequency offset parameters respectively

$$\begin{aligned} \phi_{i,k} &= (1+\zeta)(\Delta f T_u + i) - k \\ \phi_k &= \phi_{k,k} \approx \Delta f T_u + \zeta k \end{aligned} \tag{9}$$

where $si(\pi\phi_k) = \sin(\pi\phi_k)/(\pi\phi_k)$ and $si(\pi\phi_{i,k}) = \sin(\pi\phi_{i,k})/(\pi\phi_{i,k})$ are the attenuation factors, H_k is the channel transfer function (CTF) at subcarrier frequency k and $n_{l,k}$ is noise.

Modeling the irreducible ICI as an additional noise $n_{l,k}^{\Omega}$, the demodulated signal becomes

$$z_{l,k} = (e^{j\pi(1+2N_g/N)\phi_k} e^{j2\pi lN_s/N\phi_k}) si(\pi\phi_k) s_{l,k} H_k + n_{l,k}^{\Omega} + n_{l,k} \tag{10}$$

The residual local offset ϕ_k is usually small enough to approximate the attenuation factor $si(\pi\phi_k) = \sin(\pi\phi_k)/(\pi\phi_k)$ to 1 and it could be neglected. Furthermore, the time-invariant term $e^{j\pi(1+2N_g/N)\phi_k}$ can't be distinguished from the H_k. Hence, the residual phase is $2\pi lN_s/N\phi_k$, which can be rewritten as

$$\begin{aligned} \phi_l(k) &= 2\pi lN_s/N\phi_k = \underbrace{2\pi lN_s/NT_u\Delta f}_{c_l} + \underbrace{2\pi lN_s/N\zeta k}_{\delta_l k} \\ &= c_l + \delta_l k \end{aligned} \tag{11}$$

Then, sub-carrier k belonging to symbol l can be expressed as follow after FFT

$$z_{l,k} = e^{j\phi_l(k)} H_k s_{l,k} + n'_{l,k} = e^{j(c_l+\delta_l k)} H_k s_{l,k} + n'_{l,k} \tag{12}$$

where c_l is the CPE, δ_l is the STO and $n'_{l,k} = n_{l,k}^{\Omega} + n_{l,k}$ is the total noise.

3. Proposed algorithm

3.1 Existing WLS

The pilot tones in the OFDM symbols can be used to track CPE and STO, which should be performed before detection operation. In this section, we take 20 MHz bandwidth in the 802.11ac system as an example to illustrate, and 40 MHz and 80 MHz are similar. There are four pilots for 20 MHz bandwidth, whose frequency indexes are −21, −7, 7 and 21. Let $\mathrm{p}_l = [p_{l,-21} \quad p_{l,-7} \quad p_{l,7} \quad p_{l,21}]^T$ be the 4×1 pilot vector, and $\mathrm{Z}_l = [z_{l,-21} \quad z_{l,-7} \quad z_{l,7} \quad z_{l,21}]^T$ denotes the 4×1 data vector corresponding to the pilot subcarriers in the *lth* received symbol. Besides, the 4×1 estimated channel response vector corresponding to the pilot subcarriers is $\mathrm{h}_P = [h_{-21} \quad h_{-7} \quad h_7 \quad h_{21}]^T$. Then,

$$\mathrm{Z}_l = \mathrm{P}_l \mathrm{H}_P \varphi_l + \mathrm{n}_l \tag{13}$$

where $\varphi_l = [e^{j\phi_l(-21)} \quad e^{j\phi_l(-7)} \quad e^{j\phi_l(7)} \quad e^{j\phi_l(21)}]^T$, $\mathrm{P}_l = diag(\mathrm{p}_l)$, $\mathrm{H}_P = diag(\mathrm{h}_P)$ and n_l denotes the noise vector. A desired performance can be achieved by widely used WLS, but with a high calculation complexity.

The existing LS estimation of φ_l is

$$\hat{\varphi}_l = ((\mathrm{P}_l\mathrm{H}_P)^H\mathrm{P}_l\mathrm{H}_P)^{-1}(\mathrm{P}_l\mathrm{H}_P)^H\mathrm{Z}_l \tag{14}$$

It is known that

$$\angle\hat{\varphi}_l = \begin{bmatrix} \hat{\phi}_l(-21) \\ \hat{\phi}_l(-7) \\ \hat{\phi}_l(7) \\ \hat{\phi}_l(21) \end{bmatrix} = \begin{bmatrix} 1 & -21 \\ 1 & -7 \\ 1 & 7 \\ 1 & 21 \end{bmatrix} \begin{bmatrix} \hat{c}_l \\ \hat{\delta}_l \end{bmatrix} = \mathrm{D}\begin{bmatrix} \hat{c}_l \\ \delta_l \end{bmatrix} \tag{15}$$

where $\hat{\phi}_l(-21)$, $\hat{\phi}_l(-7)$, $\hat{\phi}_l(7)$ and $\hat{\phi}_l(21)$ are the estimated angles of pilot subcarriers.

So, the LS estimation of c_l and δ_l can be given by

$$\begin{bmatrix} \hat{c}_l \\ \hat{\delta}_l \end{bmatrix} = (\mathrm{D}^T\mathrm{D})^{-1}\mathrm{D}^T(\angle\hat{\varphi}_l) \tag{16}$$

In order to obtain an improved estimation of $\hat{c}_l$ and $\hat{\delta}_l$, WLS is provided

$$\begin{bmatrix} \hat{c}_l \\ \hat{\delta}_l \end{bmatrix} = (\mathrm{D}^T\mathrm{W}\mathrm{D})^{-1}\mathrm{D}^T\mathrm{W}(\angle\hat{\varphi}_l) \tag{17}$$

with weighted matrix W corresponding to the channel response vector H_P.

3.2 Proposed algorithm

The WLS introduces weighted matrix to improve system performance, but it increases complexity at the same time. In order to reduce the complexity without performance penalty, we put forward SWLS with three strategies, which are CPE ML estimation, angle boundary treatment and combined scheme of pair pilots.

1) CPE ML estimation

When $\delta_l = 0$, Eq. (13) can be simplified as

$$\mathrm{Z}_l = e^{jc_l}\mathrm{P}_l\mathrm{H}_P\mathrm{E} + \mathrm{n}_l = e^{jc_l}\mathrm{P}_l\mathrm{h}_P + \mathrm{n}_l \tag{18}$$

From [18], we know the ML estimation of e^{jc_l} is

$$e^{j\hat{c}_l} = \arg\min \|\mathrm{Z}_l - e^{j\hat{c}_l}\mathrm{P}_l\mathrm{h}_P\|^2 = \frac{(\mathrm{P}_l\mathrm{h}_P)^H\mathrm{Z}_l}{\|\mathrm{P}_l\mathrm{h}_P\|^2} \tag{19}$$

When $\delta_l = 0$, we can get the ML estimation of c_l

$$\hat{c}_l = \angle\{(\mathrm{P}_l\mathrm{h}_P)^H\mathrm{Z}_l\} \tag{20}$$

In WLANs, the CFO and STO are derived from the same reference oscillator, so they have the same value. From Eq. (11), we have

$$\begin{aligned} |\delta_l p/c_l| &= |\zeta p/(T_u\Delta f)| = |\zeta p/(T_u\zeta c_f e_f)| \\ &= |p/(T_u c_f e_f)| < 0.06 \end{aligned} \tag{21}$$

where $p \in \{-21, \ -7, \ 7, \ 21\}$ denotes the frequency index of pilot subcarrier, $T_u = 3.2\,\mu\mathrm{s}$ is the useful symbol time, $c_f = 5.8\,\mathrm{G}$ is the central frequency and $e_f = 2\%$ is the residual carrier frequency.

So we can use Eq. (20) to calculate $\hat{c}_l$, which means that the matrix operations used in WLS can be replaced by an arctangent function. This CPE ML estimation carries out the vector merging before arctangent calculation, which will reduce the information loss of multiple arctangent operations and thus improve the estimation performance.

In practice, we use coordination rotation digital computer (CORDIC) [29] to calculate arctangent.

2) angle boundary treatment

In WLANs, $N_s/N \leq 1.25$ and ζ is within ±40 ppm, so Eq. (22) is satisfied

$$|\phi_{l+1}(p) - \phi_l(p)| = |2\pi N_s/N(T_u\Delta f + \zeta p)| < \pi \tag{22}$$

When $\hat{\phi}_{l+1}(p)$ and $\hat{\phi}_l(p)$ belong to the different sides of the boundary, we should turn $\hat{\phi}_{l+1}(p)$ to the same side of $\hat{\phi}_l(p)$. The scheme is shown as the following Table I.

Table I. The adjustment scheme of boundary angle.

$\hat{\phi}_l^{in}(p)$ and $\hat{\phi}_{l+1}^{in}(p)$		$\hat{\phi}_{l+1}^{out}(p)$
$\hat{\phi}_l(p) \geq 0$	$\hat{\phi}_{l+1}(p) \geq 0$	$\hat{\phi}_{l+1}(p)$
$\hat{\phi}_l(p) \leq 0$	$\hat{\phi}_{l+1}(p) \leq 0$	$\hat{\phi}_{l+1}(p)$
$\pi \geq \hat{\phi}_l(p) \geq \pi/2$	$-\pi/2 \geq \hat{\phi}_{l+1}(p) \geq -\pi$	$\hat{\phi}_{l+1}(p) + 2\pi$
$-\pi/2 \geq \hat{\phi}_l(p) \geq -\pi$	$\pi \geq \hat{\phi}_{l+1}(p) \geq \pi/2$	$\hat{\phi}_{l+1}(p) - 2\pi$

3) combined scheme of pair pilots

For WLS, the angles of different pilot sub-carriers are handled separately. In order to reduce the complexity, we divide the four pilots into two group of $\hat{\phi}_l(\pm 7)$ and $\hat{\phi}_l(\pm 21)$. Then, Eq. (15) can be rewritten

$$\angle\tilde{\varphi}_l = \begin{bmatrix} \hat{\phi}_l(21) - \hat{\phi}_l(-21) \\ \hat{\phi}_l(7) - \hat{\phi}_l(7) \end{bmatrix} = \begin{bmatrix} 42 \\ 14 \end{bmatrix}\hat{\delta}_l = \tilde{\mathrm{D}}\hat{\delta}_l \tag{23}$$

According to the state information of channel, $\hat{\delta}_l$ is calculated as

$$\hat{\delta}_l = (\tilde{\mathrm{D}}^T\mathrm{W}_\mathrm{s}\tilde{\mathrm{D}})^{-1}\tilde{\mathrm{D}}^T\mathrm{W}_\mathrm{s}(\angle\tilde{\varphi}_l) \tag{24}$$

where the W_s is the combining coefficient related to the channel information of the pair pilots.

$$\mathrm{W}_\mathrm{s} = \begin{bmatrix} \|\tilde{H}_{21}\|^2 & \\ & \|\tilde{H}_7\|^2 \end{bmatrix} \tag{25}$$

In this paper, we have the weighted W_s as Eq. (26).

$$\begin{cases} \tilde{H}_{21} = (abs(re(H_{21})) + abs(re(H_{-21}))) \\ \qquad + j(abs(im(H_{21})) + abs(im(H_{-21}))) \\ \tilde{H}_7 = (abs(re(H_7)) + abs(re(H_{-7}))) \\ \qquad + j(abs(im(H_7)) + abs(im(H_{-7}))) \end{cases} \tag{26}$$

Once $\hat{c}_l$ and $\hat{\delta}_l$ are determined, we can do the correction straight forward according to Eq. (12).

4. Numerical results

4.1 Comparison of estimation complexity

In this section, we present the complexity comparison of related methods in Table II. The complexity values are obtained based on the parameters of 20 MHz bandwidth in the 802.11ac system. In order to illustrate complexity reduction effect of the combined scheme of pair pilots, SWLS with three strategies and SWLS II with only two strategies (the CPE ML estimation and the angle boundary treatment) are provided for comparison.

The calculation of $\hat{c}_l$ by the CPE ML estimation requires 14 additions, 16 multiplications and 1 arctangent operation. The calculation of $\hat{\delta}_l$ by the combined scheme of pair pilots needs 6 additions, 8 multiplications, 1 division and 4 arctangent operations, while 24 additions, 12 multiplications, 8 divisions and 4 arctangent operations are needed without the combined scheme of pair pilots. The angle boundary treatment is done through 2 sign judgments, 4 size comparators and 2 additions, so nearly 6 additions are needed.

Finally the SWLS totally needs 26 additions, 24 multiplications, 1 division, 5 arctangent operations, while the SWLS II needs 44 additions, 28 multiplications, 8 divisions and 5 arctangent operations.

Table II. Comparison of estimation complexity for different methods

	CPE	SRPCM	WLS	SWLS	SWLS II
addition	14	34	39	26	44
multiplication	16	28	40	24	28
division	0	8	8	1	8
arctangent	1	0	4	5	5

As shown in Table II, CPE is the simplest method, but it ignores the influence of STO. As the arctangent calculation is easier than division, the SWLS has lower complexity than SRPCM. Compared to the WLS algorithm, more than 40 percent of complexity is reduced with SWLS. Thanks to the combined scheme of pair pilots, the complexity of SWLS has decreased more than 15 percent compared to SWLS II.

4.2 Comparison of PER performance

The PER performance of SWLS and SWLS II is investigated and compared to CPE, SPRCM and WLS. The system model is according to the IEEE 802.11ac standard, where the performance under AWGN channel and frequency selective channel, taking TGn B [30] as an example, is simulated. Transmission of 4096 byte bits per burst is assumed, using three different data rates: 19.5 Mbps, 39 Mbps and 65 Mbps defined in the 802.11ac. The CFO and STO equal to 10 ppm and 40 ppm are used in the simulation, and a residual carrier frequency is 2 percent after synchronization. The PN is selected together, with model as given in [11]. Simulation parameters are shown in Table III.

Table III. PER simulation parameters

Center frequency	5.8 GHz
Bandwidth	20 MHz
Data rate	mcs 2: 19.5 Mbps, mcs 4: 39 Mbps and mcs 7: 65 Mbps
Data Length	4096 [byte]
CFO and STO	10 ppm and 40 ppm
PN	$a = 7$, $b = 4$, $c = 11$
Channel model	AWGN and TGn B

PER smaller than 10^{-1} is required in IEEE 802.11ac system, so signal to noise ratio (SNR) for PER equal to 10^{-1} can be an indication of algorithm performance. The PER performance comparison among SWLS (SWLS), SWLS II (SWLS II), CPE (CPE), SPRCM (SPR) and WLS (WLS) under AWGN with CFO and STO equal to 10 ppm and 40 ppm is shown in Fig. 2 and Fig. 3 respectively, and the PER performance comparison under TGn B is shown in Fig. 4 and Fig. 5.

It can be found when CFO and STO are 10 ppm, the PER performance of MCS 7 for CPE becomes worse than the SWLS method under TGn B (Fig. 4). Furthermore, when CFO and STO come to 40 ppm, PER degrades a lot

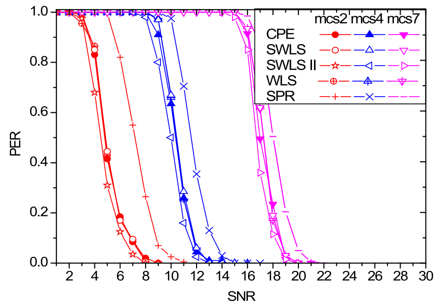

Fig. 2. PER performance under AWGN for CFO/STO equal to 10 ppm

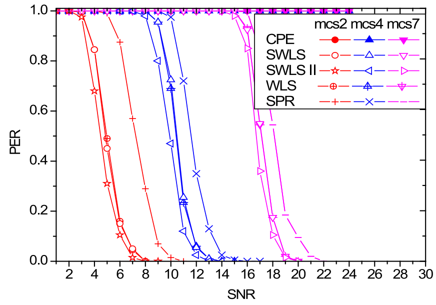

Fig. 3. PER performance under AWGN for CFO/STO equal to 40 ppm

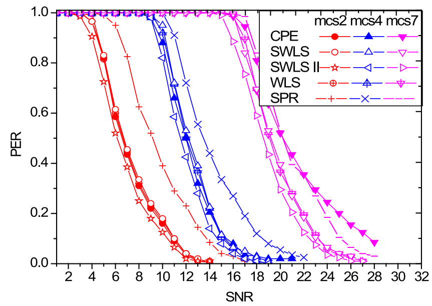

Fig. 4. PER performance under TGn B for CFO/STO equal to 10 ppm

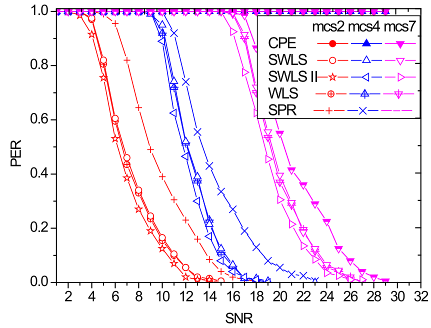

Fig. 5. PER performance under TGnB for CFO/STO equal to 40 ppm

with CPE and is almost 100%, but it is still working with SWLS (Fig. 3 and Fig. 5).

As show in Fig. 2, 3, 4 and 5, when PER is 10^{-1}, SWLS achieves better performance gain than SPR for all cases. Minimum 1 dB performance superior is achieved by mcs7 in AWGN and maximum 3 dB performance superior is achieved by mcs4 in TGn B.

Compared to WLS, the required SNR for SWLS is no more than 0.1 dB in all scenarios, which means the SWLS has almost identical performance with WLS.

As show in Fig. 2, 3, 4 and 5, when PER is 10^{-1}, SWLS II achieves better performance gain than SWLS and WLS for all cases. Nearly 0.5 dB performance superior is achieved, which means CPE ML estimation and angle boundary treatment can give performance gain.

5. Conclusion

A SWLS method has been presented in this paper, which aims to reduce the complexity without much system performance loss. Simulation result shows that aided with CPE ML estimation, angle boundary treatment and combined scheme of pair pilots, the SWLS method has a low complexity and is robust to residual CFO and STO.

References

[1] IEEE Std 802.11n-2009, Part 11: Wireless LAN Medium Access control (MAC) and Physical Layer (PHY) specifications, 2013.
[2] IEEE Std 802.11ac TM/D7.0, Part 11: Wireless LAN Medium Access control (MAC) and Physical Layer (PHY) specifications, 2013.
[3] R. V. Nee and R. Parad: *OFDM for Wireless Multimedia Communications* (Artech House, Boston, MA, 2002).
[4] J. Heiskala and J. Terry: *OFDM Wireless LANS: A Theoretical and Practical Guide* (Sams, Indianapolis, IN, 2002).
[5] M. Krstic, *et al.*: "Optimized low power synchronizer design for the IEEE 802.11a standard," ICASSP on Acoustics, Speech and Signal **2** (2003) 333 (DOI: 10.1109/ICASSP.2003.1202362).
[6] B. Ai, *et al.*: "Frequency offset estimation for OFDM in wireless communications," IEEE Trans. Consum. Electron. **50** (2004) 73 (DOI: 10.1109/TCE.2004.1277843).
[7] S. H. Son and J. T. Kim: "A robust coarse symbol timing synchronization for OFDM systems in multi-path fading channel," 2008 IEEE International Symposium on Consumer Electronics (2008) 1 (DOI: 10.1109/ISCE.2008.4559493).
[8] H. Abdzadeh-Ziabari, *et al.*: "Robust timing and frequency synchronization for OFDM systems," IEEE Trans. Veh. Technol. **60** (2011) 3646 (DOI: 10.1109/TVT.2011.2163194).
[9] D. Chong, *et al.*: "Robust estimators for frequency offset of OFDM in non-Gaussian noise," IEICE Electron. Express **8** (2011) 1412 (DOI: 10.1587/elex.8.1412).
[10] T. Pham, *et al.*: "Efficient integer frequency offset estimation architecture for enhanced OFDM synchronization," IEEE Trans. Very Large Scale Integr. (VLSI) Syst. **24** (2016) 1412 (DOI: 10.1109/TVLSI.2015.2453207).
[11] P. Robertson, *et al.*: "Analysis of the effects of phase noise in OFDM system," ICC on Communications **3** (1995) 1652 (DOI: 10.1109/ICC.1995.524481).
[12] S. Q. Zhao, *et al.*: "Analysis of joint effect of phase noise, IQ imbalance and amplifier nonlinearity in OFDM system," WCSP on Wireless Communications and Signal Processing (2013) 1 (DOI: 10.1109/WCSP.2013.6677201).
[13] P. Mathecken, *et al.*: "Performance analysis of OFDM with wiener phase noise and frequency selective fading channel," IEEE Trans. Commun. **59** (2011) 1321 (DOI: 10.1109/TCOMM.2011.030411.100401).
[14] G. Miriyala, *et al.*: "Joint estimation of channel response, frequency offset and phase noise in OFDM systems," ICICCS on Intelligent Computing and Control Systems (2018) 1299 (DOI: 10.1109/ICCONS.2018.8663086).
[15] J. M. Speth, *et al.*: "Optimum receiver design for wireless broadband systems using OFDM-part I," IEEE Trans. Commun. **47** (1999) 1668 (DOI: 10.1109/26.803501).
[16] J. M. Speth, *et al.*: "Optimum receiver design for OFDM-based broadband transmission II. A case study," IEEE Trans. Commun. **49** (2001) 571 (DOI: 10.1109/26.917759).
[17] L. Rugini and P. Banelli: "BER of OFDM systems impaired by carrier frequency offset in multipath fading channels," IEEE Trans. Wireless Commun. **4** (2005) 2279 (DOI: 10.1109/TWC.2005.853884).
[18] J. Liu and J. Li: "Parameter estimation and error reduction for OFDM-based WLANs," IEEE Trans. Mobile Comput. **3** (2004) 152 (DOI: 10.1109/TMC.2004.11).
[19] O. Weikert: "Joint estimation of carrier and sampling frequency offset, phase noise, IQ offset and MIMO channel for LTE advanced UL MIMO," SPAWC in Wireless Communications (2013) 520 (DOI: 10.1109/SPAWC.2013.6612104).
[20] Y. Cao, *et al.*: "A novel receiver design and maximum-likelihood detection for distributed MIMO systems in presence of distributed frequency offsets and timing offsets," IEEE Trans. Signal Process. **66** (2018) 6297 (DOI: 10.1109/TSP.2018.2875391).
[21] A. Troya, *et al.*: "Low-power VLSI implementation of the inner receiver for OFDM-based WLAN systems," IEEE Trans. Circuits Syst. I, Reg. Papers **55** (2008) 672 (DOI: 10.1109/TCSI.2007.913732).
[22] J. I. Montojo, *et al.*: "Effects of imperfections on the performance of OFDM systems," IEEE Trans. Commun. **57** (2009) 2060 (DOI: 10.1109/TCOMM.2009.07.070452).
[23] Y. H. You, *et al.*: "Accurate pilot-aided sampling frequency offset estimation scheme for DRM broadcasting systems," IEEE Trans. Broadcast. **56** (2010) 558 (DOI: 10.1109/TBC.2010.2056253).
[24] A. Troya, *et al.*: "Efficient inner receiver design for OFDM-based WLAN systems: Algorithm and architecture," IEEE Trans. Wireless Commun. **6** (2007) 1374 (DOI: 10.1109/TWC.2007.348334).
[25] K.-B. Png, *et al.*: "Joint carrier and sampling frequency offset estimation for MB-OFDM UWB system," RWS (2008) 29 (DOI: 10.1109/RWS.2008.4463420).
[26] I. Hwang, *et al.*: "Frequency and timing period offset estimation technique for OFDM systems," Electron. Lett. **34** (1998) 520 (DOI: 10.1049/el:19980386).
[27] A. Troya, *et al.*: "Simplified residual phase correction mechanism for the IEEE 802.11a standard," IEEE 58th Vehicular Technology Conference (2003) 1137 (DOI: 10.1109/VETECF.2003.1285199).
[28] P. Y. Tsai, *et al.*: "Joint weighted least-squares estimation of carrier-frequency offset and timing offset for OFDM systems over multipath fading channels," IEEE Trans. Veh. Technol. **54** (2005) 211 (DOI: 10.1109/TVT.2004.838891).
[29] H.-T. Nguyen, *et al.*: "Low-resource low-latency hybrid adaptive CORDIC with floating-point precision," IEICE Electron. Express **12** (2015) 20150258 (DOI: 10.1587/elex.12.20150258).
[30] G. B, *et al.*: "TGac Channel Model Addendum Support Material," IEEE 802.11-09/06/0569r0 (2009).